J Nanopart Res (2012) 14:1261
DOI 10.1007/s11051-012-1261-2

RESEARCH PAPER

Damping effect of the inner band electrons on the optical absorption and bandwidth of metal nanoparticles

Lawrence Ochoo · Charles Migwi · John Okumu

Received: 18 January 2012 / Accepted: 20 October 2012 / Published online: 9 November 2012

Abstract Conflicts and discrepancies around nanoparticle (NP) size effect on the optical properties of metal NPs of sizes below the mean free path of electron can be traced to the internal damping effect of the hybrid resonance of the inner band (IB) and the conduction band (CB) electrons of the noble metals. We present a scheme to show how alternative mathematical formulation of the physics of interaction between the CB and the IB electrons of NP sizes <50 nm justifies this and resolves the conflicts. While a number of controversies exist between classical and quantum theories over the phenomenological factors to attribute to the NP size effect on the absorption bandwidth, this article shows that the bandwidth behavior can be well predicted from a different treatment of the IB damping effect, without invoking any of the controversial phenomenological factors. It finds that the IB damping effect is mainly frequency dependent and only partly size dependent and shows how its influence on the surface plasmon resonance can be modeled to show the influence of NP size on the absorption properties. Through the model, it is revealed that strong coupling of IB and CB electrons drastically alters the absorption spectra, splitting it into distinctive dipole and quadrupole modes and even introduce a behavioral switch. It finds a strong overlap between the IB and the CB absorptions for Au and Cu but not Ag, which is sensitive to the NP environment. The CB modes shift with the changing refractive index of the medium in a way that can allow their independent excitation, free of influence of the IB electrons. Through a hybrid of parameters, the model further finds that metal NP sizes can be established not only by their spectral absorption peak locations but also from a proper correlation of the peak location and the bandwidth (FWHM).

Keywords Metal nanoparticles · Inner band damping effect · Plasmon resonance · Eigenmodes · FWHM absorption of NPs

L. Ochoo (✉) · C. Migwi · J. Okumu
Physics Department, Kenyatta University,
P.O. Box 3844, Nairobi 00100, Kenya
e-mail: lawijapuonj@yahoo.com

Introduction

Particles of metals in the nanoscale (1–100 nm), commonly known as nanoparticles (NPs), exhibit size-dependent enhanced optical, opto-electronic, and photothermal properties which have made them attractive for industrial, electronic data transfer and storage, biomedical diagnostics and photothermal therapy on cancer cells, among others. As the interest over their potential applications grows, the dependence of their optical properties on the hybrid contribution of the conduction band (CB) and the inner band (IB, especially the d-band) electrons is yet to be well established within the framework of both the classical and the quantum theories. Their optical properties, however,

have largely been attributed to the collective oscillations of the CB electrons, known as the surface plasmon resonance (SPR) (Gharibshahi and Saion 2010). Hitherto, the challenge has been how the influence of the IB electrons can be introduced into a mathematical model to correctly predict the NP size effect on their optical properties, especially in the size range below the mean free path (MFP) of electron, which is ~40–50 nm in gold, silver, and copper. From the theories of the existing models, the IB contribution enters a model through the dielectric function of a metal (Pinchuk et al. 2004). Another challenge has been how to resolve conflicts arising out of the fact that classical and quantum mechanical approaches employing different phenomenological theories arrive at the same mathematical law expressing inverse NP size effect ($1/R$), for sizes below ~20 nm (Kawabata and Kubo 1966; Kreibig and Genzel 1985). This makes it difficult to ascertain the adequacy of a model or its descriptive parameters on the basis of the property–size relation or the assumed phenomenal mechanisms, especially when it fails to give accurate prediction of the size effect. As a result, uncertainties hang over the understanding of the exact optical property–size correlation and their ultimate potential applications. This is better understood from the conflicting information about what the most effective gold NP size for the photothermal destruction of cancer should be, which Zharov et al. (2003) declare to be sizes in the range of 10–30 nm, while Link and El-Sayed (1999a, b) also report ~40 nm to be very effective. Several efforts have been made to unveil models which can provide full description of the optical properties of the NPs of Ag, Au, and Cu, from the values of the parameters of their bulk form, especially the dielectric functions (Kreibig and Genzel 1985; Pinchuk et al. 2004). Mie (1908) was the first to make attempt to describe the optical properties of metal NPs in terms of the parameters of their bulk materials, based on the oscillations of the CB electrons (SPR). However, serious conflicts and discrepancies have since been realized between the theoretical and the experimental results, for the NP sizes below 20 nm. One major area of conflict has been that of the experimentally observed anomalous absorption bandwidth behavior as the particle size reduces below the MFP. This is where the absorption bandwidth decreases with reducing NP size then starts increasing on a further reduction of the NP size. The existing models do not seem to agree on the phenomenological mechanisms responsible for this (Kreibig and Genzel 1985; Kawabata and Kubo 1966; Pinchuk et al. 2004).

Mie theory

The common models for the understanding of the factors responsible for the optical properties of metal NPs, of the size below the MFP, have been based on the Mie theory (Kreibig and Vollmer 1995; Pinchuk et al. 2004; Jain et al. 2006). The full Mie theory (Mie 1908) expresses the light extinction cross section of homogeneous spherical particles as infinite series of the polynomials of excitable electric and magnetic multipoles. Higher polynomial terms are meant to address issues associated with larger NP size, basically above the electron's MFP, like the onset of the contributions of the higher resonances or multipolar modes (Jain et al. 2006; Mie 1908). The theory easily describes red shifts and broadening of the absorption spectrum of larger particles as the size increases, as well as the occurrence of the multipolar modes (quadrupole and octupole). When the NP size becomes much smaller than the wavelength of the exciting light ($2R < \lambda/10$), the magnetic multipoles are ignored and the light extinction (absorption + scattering) is considered to be dominated by the electric dipoles and the theory reduces to the form commonly known as the Mie's dipole approximation model whose absorption cross section is given by Eq. 1. In this approximation, the model still assumes that the dielectric constants of the bulk materials (>50 nm) can adequately describe and predict the optical properties of NP sizes below the MFP. This became the starting point of the conflicts encountered between the theories in this field

$$\sigma_{\text{abs}} = \frac{24\pi^2 R^3 \varepsilon_{\text{m}}^{3/2}}{\lambda_0} \frac{\varepsilon_2}{(\varepsilon_1 + 2\varepsilon_{\text{m}})^2 + \varepsilon_2^2}, \quad (1)$$

where R is the particle radius, λ_{o} is the wavelength of the absorbing radiation, ε_{m} is the dielectric constant of the medium, ε_1 and ε_2 are the real and imaginary parts of the dielectric constants of the bulk material. For small ε_2, absorption peak is realized when $\varepsilon_1 = -2\varepsilon_{\text{m}}$.

Because most technologically important optical properties of interest involve NP sizes below 50 nm, much of the research interests currently focus on the NP size effects of that regime and, as a result, the inadequacy and review of the Mie's dipole

approximation mode (Kreibig and Genzel 1985; Pinchuk et al. 2004). In the framework of the dipole approximation model, Eq. 1, and by its parameters, NP size was only expected to influence the absorption intensity but not the peak position or the bandwidth. Experimental observations, however, have shown strong size dependence of both the absorption bandwidth and the peak location (Link and El-Sayed 1999a, b). For the NP sizes below the MFP, the peak position has been reported to show a blue shift with reducing NP size and the bandwidth exhibits the inverse law $-1/R$ in the region below $\sim$20 nm (Link and El-Sayed 1999a, b). The Mie's dipole approximation model has been found inadequate because it does not show the $(1/R)$ dependence of the bandwidth behavior. In addition, it has been criticized as a mathematical model lacking underlying phenomenological mechanisms described by its parameters and that it may not be suitable for use as an analytical tool (Etchegoin et al. 2006; Gharibshahi and Saion 2010; Nordlander and Prodan 2003). The discrepancies between the predictions of Eq. 1 and the experimental observations, especially the inverse law $(1/R)$, have since been assumed to be a consequence of some intrinsic size effect on the dielectric function, which the dipole approximation model overlooks (Kreibig and Vollmer 1995; Pinchuk et al. 2004).. According to Kreibig and Genzel (1985) it is due to an increased electron-surface scattering, resulting from the reduced MFP of electron as the NP size reduces. On the basis of this, he obtained the associated damping effect in the form of Eq. 2

$$\gamma = \gamma_\infty + A\frac{v_F}{R}, \tag{2}$$

where γ_∞ is the bulk damping constant, v_F is the velocity of the CB electron at the Fermi energy, A is a constant depending on the nature of scattering.

On applying Eq. 2, Pinchuk et al. (2004) modified the Mie's dipole approximation model, Eq. 1, on the basis of the electron-surface scattering and its influence on the dielectric constants, obtaining expression given by Eq. 3

$$\sigma_{abs} = \frac{24\pi^2 R^3 \varepsilon_m^{3/2}}{\lambda_0}\frac{1}{[1+\varepsilon_1+2\varepsilon_m]} \times \frac{\Omega^2\gamma\omega^2 + k\omega^3(\omega^2+\gamma^2)}{\left(\Omega^2-\omega^2+k\omega\gamma\right)^2+(\gamma\omega+\kappa\omega^2)^2}, \tag{3}$$

where

$$\Omega = \frac{\omega_p}{[1+\varepsilon_1+2\varepsilon_m]^{1/2}}, \quad k = \frac{\varepsilon_2}{[1+\varepsilon_1+2\varepsilon_m]},$$

where ω_p is the plasmon resonance freq, ω is the frequency of light and other symbols have the same meanings as before.

However, even with the inclusion of the intrinsic size effect into the Mie theory, the model improves but still underestimates the absorption bandwidths (Pinchuk et al. 2004; Yeshchenko et al. 2007). This may be interpreted to mean the existence of additional damping mechanism(s) whose descriptive parameters have not been included or just a general weakness of the model. It has been argued that the inverse law $(1/R)$ can also be arrived at by assuming some other effects, such as the chemical nature of the NP surrounding, without invoking the electron-surface scattering damping effect, as seen in the case of Persson and (1993) or Kawabata and Kubo (1966). From a quantum mechanical approach, Kawabata and Kubo (1966) found the inverse law $(1/R)$ by assuming the excitation of new surface Eigenmodes as the NP size reduces. These arguments have led to conflicts about what should be the correct phenomenological mechanisms responsible for the inverse law. The conflicts which started from a simple issue of whether the parameters for the bulk metals can be employed in the theoretical characterization of their NPs, as implied in the model of Eq. 1, has since become an issue of the physics of the mechanisms involved and the parameters of association (classical or quantum). The biggest challenge, therefore, is why the same mathematical law for property description should lend itself to different independent phenomenological interpretations which would leave researchers struggling to balance between the theories, adopting one or the other depending on the convenience or simplicity one finds for the discussion of experimental results.

Experimentally, the properties of NPs of a metal(s) are very much different from those of their bulk materials and a number of parameters of the bulk materials are not a direct indicator of the aspects of spectral similarity or differences observed in the absorption spectra of different noble metals (Ag, Au, and Cu). A good example is where the electron density and Fermi energy velocity for the bulk metals of Au and Ag are almost equal, than they are to Cu, but the experimental light absorption characteristics of Au NPs are closer and similar to Cu NPs than Ag. It is,

however, not clear whether this argument should be used to dismiss the possibility that parameters of a bulk material can still give accurate predictions of property behavior and magnitude as had been anticipated for Eq. 1, if the correct microscopic phenomenological mechanisms in play are identified.

In the proposed model of this article, it is held that the cause of the failure and conflict between the above-mentioned phenomenological theories may be a consequence of the physics, associative parameters and the mathematical formalism employed in describing the interaction between electrons in metal NPs and the electromagnetic waves. That a general phenomenological theory, whose model resolves the conflicts and proves the size-dependent anomalous absorption bandwidth and peak shift behavior in terms of parameters of the bulk materials, would require a different approach. Of great significance to this article is that the modified Mie theory, Eq. 3, suggests a hybrid of parameters (ε, ω_p, and ω), which could be an indicator that there has been inadequacy in the Mie's dipole approximation model even in terms of the parameters for the prediction of NP size-dependent absorption characteristics. However, from the fact that even the modified model still underestimates the absorption bandwidth, it may be possible that it is not just the size dependence of the dielectric constant that causes the discrepancy between the Mie's dipole approximation model and the experimental results. That if the correct phenomenon and parameters were established then even the dielectric constants of the bulk materials could still have predicted the correct NP absorption characteristics.

Behind the aforementioned inadequacies and conflicts, one thing is certain. That the current level of interest toward the potential optical applications of the NPs of Au, Ag, and Cu demands a clear phenomenon-based model as a tool for correlating, predicting, and monitoring application-related dynamics involving NP size and systems. Attempts have been made to correlate NP size and shapes with the absorption peak locations, to aid in the NP size characterization and selection for various applications, however, the correlation results have been probabilistic and merely suggestive of the size regimes (Etchegoin et al. 2006; Solomon et al. 2007). Currently, the only reliable means of monitoring size and dynamics in various systems is by transmission electron microscope (TEM). With a very predictive model, even simple spectroscopic measurements can be used to predict NP size and agglomeration dynamics as demonstrated in this article.

Scheme of the proposed model

The general perception is that when electromagnetic field is applied to a small particle the electrons cloud is displaced as a unit, leading to a dipole moment in which a single particle can be represented by a single dipole moment, Fig. 1a. This picture assumes that the whole center of the negative charge is displaced in one direction once the electrons cloud of the CB electrons is displaced.

In a dynamic system, and when the CB electrons are not so much delocalized to be screened from the positive ions, this may not be possible at all frequencies. That is, if only part of the CB electrons are free as in the Drude model (Kittel 1986) while part of the cloud and the IB electrons experience strong positive ion effect, then the IB electrons are expected to interact with the CB electrons in their oscillatory motion. Depending on how strong the IB and CB electrons couple in this motion, the cloud associated with the IB electrons would be out of phase with the cloud of the near-free CB electrons at some frequencies, especially at higher frequencies of the driving external force. Because of this, the proposed scheme introduces two concentric electron clouds (IB and CB), whose centers of negative charge may be or may not be in phase, depending on the electron density and the frequency response of each cloud, Fig. 1b. This is also expected to depend on the metal type and the kinds of interband transitions taking place. This would have effect on the overall polarizability, hence, the absorbed energy and absorption peak locations. At low frequencies, near-electrostatic state, the centers of charge of the two clouds would be in phase, therefore, making one heavy cloud pushed by the external electric field due to light, in resonance. For this case, the displacement would be expected to be the highest and so would be the restoring force and the absorption. Thus, the polarization (P) can be approximated to the electrostatic state, Eq. 4

$$P = \alpha E_{\text{int}}, \tag{4}$$

where E_{int} is the electric field resulting from the polarization of the particle.

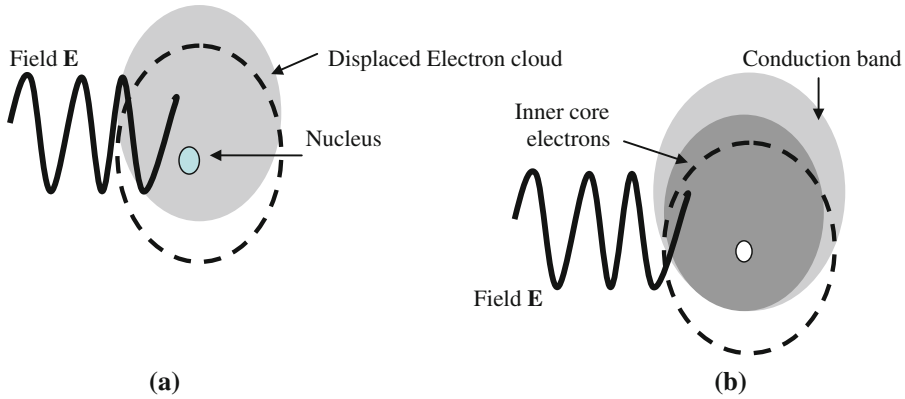

Fig. 1 Interaction between the IB and CB electrons with electromagnetic field

As the frequency increases, the IB electrons cloud and the CB electrons start leaving each other (out of phase), with the cloud of the IB electrons having small and incoherent displacements compared to the CB electrons. The out of phase oscillation is expected to cause damping on the oscillation of the CB electrons cloud, lower the polarizability and even cause a split in the absorption spectrum, depending on the phase difference. As the frequency increases further, the CB electrons cloud is expected to follow the oscillating force closely than the IB electrons. When the frequency becomes quite high, the IB electrons cloud is likely to be much out of phase with the CB electrons. Thus, depending on the coupling strength between the CB and the IB electrons clouds, the IB electrons would draw a substantial portion of energy from the CB, damping the SPR heavily and even channeling part of the energy to interband transition of the d-band electrons. It would then be the CB electrons that contribute significantly to the dynamic polarization of the NPs. Thus, the overall particle polarization is determined largely by the magnitude of the frequency-dependent damping, brought about by the IB electrons and, in the absence of external damping factors, it permits the mathematical formulation for the dynamic state to be expressed in the form of Eq. 5

$$P = [\alpha - \alpha(\omega)]E_{\text{int}}, \tag{5}$$

where α is the polarizability at very low frequency (near electrostatic state), while $\alpha(\omega)$ is the frequency-dependent part which increases with increasing frequency. Thus, increase in the frequency reduces the polarization, leading to an inverse law which can be expressed by Eq. 6

$$P = \frac{1}{\alpha'(\omega)}E_{\text{int}} \quad \text{where } 1/\alpha'(\omega) = [\alpha - \alpha(\omega)]. \tag{6}$$

The magnitude of polarization (**P**) of a particle determines the electric field inside and near the particle surface. If the dipole moment of two charges of charge q each whose centers are separated by **x** is $q\mathbf{x}$, then for a group of N atoms each of nuclear charge Ze, whose centre of the electrons cloud is displaced by x, the polarization, **P** becomes $(ZeNx)$, hence, Eq. 6 leads to Eq. 7.

$$E_{\text{int}} = ZeN\alpha'(\omega)x \tag{7}$$

The displacement x can be expressed in terms of the incident electric field of the driving force E_o and the displaceable electrons cloud whose bulk is contributed by the free CB electrons. Thus, if n electrons per atom are donated to the CB then the displaceable free electrons, per atom, is ne. As stated earlier, the displacement x is determined by the free electrons but with the damping effect of the IB electrons; therefore, from the general differential equation for a damped harmonic oscillator, x is obtained in the form of Eq. 8.

$$x = \frac{neE_0}{m}\frac{1}{\left[\left(\omega_p^2 - \omega^2\right)^2 + \gamma^2\omega^2\right]^{1/2}} \tag{8}$$

Introducing Eq. 8 into Eq. 7 leads to

$$E_{\text{int}} = \frac{Ze(Nne)\alpha'(\omega)}{m}\frac{E_0}{\left[\left(\omega_p^2 - \omega^2\right)^2 + \gamma^2\omega^2\right]^{1/2}}$$

The term (Nne) represents charge density and can be replaced with (ρ).

The Clausius–Mossotti formula (Kittel 1986; Patil 1984), relating polarizability to macroscopic dielectric constants, for a spherical particles, is assumed for $\alpha'(\omega)$.

$$N\alpha'(\omega) = 3\varepsilon_m\left(\frac{\varepsilon_p - \varepsilon_m}{\varepsilon_p + 2\varepsilon_m}\right),$$

where ε_m and ε_p are the dielectric functions of the medium and the absorbing particle, respectively.

The internal electric field then takes the form of Eq. 9.

$$E_{int} = \frac{3(Ze\rho)}{m}\varepsilon_m\left(\frac{\varepsilon_p - \varepsilon_m}{\varepsilon_p + 2\varepsilon_m}\right)\frac{E_0}{\left[\left(\omega_p^2 - \omega^2\right)^2 + \gamma^2\omega^2\right]^{1/2}}. \quad (9)$$

The electric field intensity can be expressed in terms of the photons flux, through the intensity (I) of light. For weak fields, the electric field intensity is related to the light intensity by Eq. 10 (Grant and Phillips 1975)

$$I = \frac{1}{2}c\varepsilon_m E^2 = \frac{1}{2}\left(\frac{\varepsilon\varepsilon_0}{\mu\mu_0}\right)^{1/2}E^2, \quad (10)$$

where $\mu = 1$ is for non-magnetic materials.

The classical light intensity gives a quantum measure of photon in terms of flux ϕ, as in Eq. 11 (Saleh and Teich 1991)

$$I = \phi\hbar\omega = \phi\frac{hc}{\lambda}, \quad (11)$$

where h is the Planck's constant and f is the light frequency.

For an absorbing NP, the incident light intensity is not equal to the absorbed intensity, due to distortion which makes the absorption cross section of a NP different from its actual physical cross section. Also, at resonance, $\omega = \omega_p$, and ω_p can be expressed as

$$\omega_p = \frac{2\pi c}{\lambda_p},$$

where λ_p corresponds to the electronic wave at resonance.

Therefore, let the incident light intensity associated with the captured photons, on a non-magnetic NP of dielectric constant ε_p be given by Eq. 12, where ϕ_p is the photon flux absorbed by a NP

$$I_p = \phi\hbar\omega = \phi_p\frac{hc}{\lambda_p} = \frac{1}{2}\left(\frac{\varepsilon_p}{\mu_0}\right)^{1/2}E^2. \quad (12)$$

Thus, the electric field associated with the absorbed photon flux would be

$$E_{int} = \sqrt{\phi_p\frac{2hc}{\lambda_p}\left(\frac{\mu_0}{\varepsilon_p}\right)^{1/2}}.$$

Similarly, that of the incident photons, within the surrounding medium, would be given by

$$E_0 = \sqrt{\phi_0\frac{2hc}{\lambda_0}\left(\frac{\mu_0}{\varepsilon_m}\right)^{1/2}},$$

where ϕ_0 is the photon flux, ε_m is the dielectric function of the medium, and λ_0 wavelength of light.

On introducing the expressions for E_{int} and E_0 into Eq. 9, the electric field enhancement equation is obtained in the form

$$\frac{E_{int}}{E_0} = \sqrt{\frac{\phi_p\lambda_0}{\phi_0\lambda_p}\left(\frac{\varepsilon_m}{\varepsilon_p}\right)^{1/2}} = \frac{3\varepsilon_m}{\varepsilon_p + 2\varepsilon_m}\frac{(Ze\rho)}{m}\frac{\varepsilon_p - \varepsilon_m}{\left[\left(\omega_p^2 - \omega^2\right)^2 + \gamma^2\omega^2\right]^{1/2}}.$$

This leads to an expression for the absorption of photons, Eq. 13

$$\frac{\phi_p}{\phi_0} = 9\left(\frac{Ze\rho}{m}\right)^2\frac{\lambda_p\varepsilon_p^{1/2}}{\lambda_0\varepsilon_m^{1/2}}\varepsilon_m^2\left(\frac{\varepsilon_p - \varepsilon_m}{\varepsilon_p + 2\varepsilon_m}\right)^2 \times \frac{1}{\left[\left(\omega_p^2 - \omega^2\right)^2 + \gamma^2\omega^2\right]}. \quad (13)$$

Considering the incident and the absorbed photon flux to depend on the particle's physical cross section (A) and its absorption cross section σ_{abs}, it can be assumed that the incident and the absorbed photon flux follow the proportionality law whose ratio can be given by Eq. 14.

From

$\phi_0 \propto A$ and $A = \pi R^2$

for a spherical particle of radius R

$\phi_0 \propto \sigma_{abs}$

$$\frac{\phi_p}{\phi_0} \approx \frac{\sigma_{abs}}{\pi R^2} = 9\left(\frac{Ze\rho}{m}\right)^2 \frac{\varepsilon_p^{1/2}}{\lambda_0} \varepsilon_m^{3/2} \left(\frac{\varepsilon_p - \varepsilon_m}{\varepsilon_p + 2\varepsilon_m}\right)^2 \times \frac{\lambda_p}{\left[\left(\omega_p^2 - \omega^2\right)^2 + \gamma^2\omega^2\right]}. \quad (14)$$

Because the maximum absorption takes place when the angular frequency of the absorbing electrons matches that of the photons (resonance), the de Broglie wavelength is assumed for λ_p, thus ($\lambda_p = h/\mu$). Through the de Broglie expression, the effect of NP confinement of electron can be introduced in terms of the 3D box model.

From

$$E = \frac{1}{2}\mu^2 + V_{(xyz)} \quad \text{and for a free particle}$$

$$\mu = \sqrt{2mE}.$$

The quantum expression for E, for a particle in a box of dimensions l_x, l_y, and l_z is

$$E = \frac{h^2}{8m}\left(\frac{n_x^2}{l_x^2} + \frac{n_y^2}{l_y^2} + \frac{n_z^2}{l_z^2}\right),$$

where n_x, n_y, n_z are the absorbing modes by axes.

Expression for the λ_p and, therefore, the absorption cross section of a NP in terms of the dimensions of the box then takes the form of Eq. 15

$$\sigma_{abs} = \frac{18\pi R^2 \varepsilon_m^{3/2}}{\lambda_0}\left[\frac{Ze\rho\varepsilon_p^{1/4}}{m}\right]^2 \left[\frac{\varepsilon_p - \varepsilon_m}{\varepsilon_p + 2\varepsilon_m}\right]^2 \frac{\Gamma}{[\omega]'}. \quad (15)$$

For the absorption, the imaginary part of the dielectric function is used for ε_p, where

$$\Gamma = \frac{l_x l_y l_z}{\left[\left(n_x l_y l_z\right)^2 + \left(n_y l_x l_z\right)^2 + \left(n_z l_x l_y\right)^2\right]^{1/2}}$$

$$[\omega]' = \left(\omega_p^2 - \omega^2\right)^2 + \gamma^2\omega^2,$$

where ω_p is the resonance frequencies of the particle electrons (not the bulk material) and ω is the light frequency.

For spherical NPs, the maximum region of confinement of the moving charge center of the electrons cloud, if the center of mass does not spill out of the particle, should be within ($2R$). A reasonable approximation, due to the increasing restoring force of the positive core as the displacement x increases, would be to let $l_x = l_y = l_z = R$. The absorption cross section Eq. 15, therefore, reduces to Eq. 16

$$\sigma_{abs} = \frac{18\pi R^3 \varepsilon_m^{3/2}}{\lambda_0}\left[\frac{Ze\rho\varepsilon_p^{1/4}}{m}\right]^2 \left[\frac{\varepsilon_p - \varepsilon_m}{\varepsilon_p + 2\varepsilon_m}\right]^2 \times \frac{1}{\left[n_x^2 + n_y^2 + n_z^2\right]^{1/2}} \frac{1}{[\omega]'}. \quad (16)$$

The mathematical model is similar in many aspects to Eq. 1, by the dielectric constant of the medium $\varepsilon_m^{3/2}$ and the term ($\varepsilon_p + 2\varepsilon_m$). Additional terms like nuclear charge (Ze), electron charge density (ρ), and excitable modes (n), angular frequencies ω_p and ω also exist. The presence of the new terms such as Z and ω_p is significant in this model. It is just beginning to emerge that the energy absorption by NP could be dependent on the atomic number of the absorbing metals (Z), Fermi energy, and the electron density (Gharibshahi and Saion 2010). Also, of very great significance is that, like the modified Mie model (Pinchuk et al. 2004), the plasmon frequency (ω_p,) appears in the equation, alongside the dielectric functions. The frequency (ω_p) is expected to be influenced by factors which would impact coherence in the motion of electrons, such as the NP size, shape, electron density, adsorbed molecules, and crystal defects among others. Therefore, ω_p becomes the window for seeing the effect that such factors would have on the absorption features of the metal NPs. Here, we consider ω_p in the range corresponding to (UV–IR). The experimental dielectric constants for Ag, Au, and Cu from Johnson and Christy (1972) are used in the testing of the model, applying the imaginary parts together with the values of γ given for Ag as 3.2×10^{13} s^{-1} and for Au as 1.69×10^{13} s^{-1}.

Equation for full width at half maximum (FWHM) and peak position

Equation for the FWHM, which is very similar to Eq. 2 also evolves from the absorption cross section Eq. 16, without invoking any additional phenomenological effect, as follows. Considering absorption cross section at resonance ($\omega = \omega_p$), Eq. 16 reduces to Eq. 17.

$$\sigma_{abs} = \frac{18\pi R^3 \varepsilon_m^{3/2}}{\lambda_0}\left[\frac{Ze\rho\varepsilon_p^{1/4}}{m^*}\right]^2 \left[\frac{\varepsilon_p - \varepsilon_m}{\varepsilon_p + 2\varepsilon_m}\right]^2 \times \frac{1}{\left[n_x^2 + n_y^2 + n_z^2\right]^{1/2}} \frac{1}{\left[\gamma\omega_p\right]^2}. \quad (17)$$

At FWHM, the absorption cross section would correspond to two light frequencies, ω_1 and ω_2.

Substituting the two frequencies into Eq. 16, in turn, and equating to half the absorption (for FWHM), Eq. 17 gives the following expressions:

$$\sigma_{\text{abs}}(\omega_1) = 1/2\sigma_{\max}$$

and

$$\sigma_{\text{abs}}(\omega_2) = 1/2\sigma_{\max}.$$

Leading to two quadratic equations, each of the form

$$\left(\omega_{\text{p}}^2 - \omega_s^2\right)^2 + \gamma^2\omega_s^2 = 2\gamma^2\omega_{\text{p}}^2 \quad \text{where } s = 1 \text{ or } 2.$$

Solving the resulting two equations for ω_1 and ω_2 and calculating $(\omega_1 - \omega_2)$, the following independent expressions are obtained:

$$\omega_1 - \omega_2 \approx \gamma \quad \text{and} \quad \omega_1 - \omega_2 \approx 2\omega_{\text{p}}.$$

The two independent solutions can be combined as in Eq. 18.

Let

$$\omega_1 - \omega_2 = a\gamma + b\left(2\omega_{\text{p}}\right), \tag{18}$$

where a and b are constants which can be determined from experimental data.

In terms of wavelength, Eq. 18 gives Eq. 19

$$\lambda_2 - \lambda_1 = \frac{\lambda_1\lambda_2}{2\pi c}\left[a\gamma + b\left(2\omega_{\text{p}}\right)\right]. \tag{19}$$

When the angular frequency ω_{p} becomes equal to that of the absorbed light, then in a 1D box of width $L \approx R$, the angular frequency may be expressed as

$$\omega_{\text{p}} = 2\pi f_{\text{p}} = 2\pi\frac{E}{h} = 2\pi\frac{Nh}{8mR^2}.$$

Therefore, for a 3D box of equal dimensions it is expressed as

$$\omega_{\text{p}} = 2\pi\frac{3Nh}{8mR^2},$$

where N represents $\left(n_x^2 + n_y^2 + n_z^2\right)$.

If we let $\lambda_1\lambda_2 \approx \lambda_{\max}^2$ ($\lambda_{\max}$ being the wavelength at maximum absorption), Eq. 19 leads to Eq. 20.

Thus,

$$\lambda_2 - \lambda_1 = \Delta\lambda = a\gamma\frac{\lambda_{\max}^2}{2\pi c} + b\frac{3\lambda_{\max}^2\pi Nh}{4\pi R^2 mc}. \tag{20}$$

Like Eq. 2, it is evident that this model predicts variation in the absorption bandwidth $\Delta\lambda$ to be partly dependent on the damping term γ and partly on the inverse of the NP size (by the surface area of a sphere $\propto$ R).Through this equation, the dependence of the peak position ($\lambda_{\max}$) on the NP size can be seen. Thus, the absorption bandwidth would depend on the energy losses due to factors associated with the parameters of the first and the second terms. The contribution of the first term would be determined mainly by the wavelength at maximum absorption and the damping term (γ) whose magnitude is based only on how free and coherent the oscillations of the CB electrons are. It is expected to be higher for larger NP sizes where the electric field of light would be non-uniform across the particle diameter, hence, incoherence in the oscillation. The second term is expected to introduce size and wavelength-dependent damping effects of the IB electrons and the excitable multipolar modes, through $4\pi R^2$ and N. Where the effect of the IB electrons is low and only the dipoles are excited, the contributions of the first and the second terms to the bandwidth broadening would be comparable. However, where the influence of the IB electrons and the multipolar modes are strong, the second term is expected to produce the dominant broadening effect and the contribution of (γ) can be considered negligible. Where the bandwidth is brought about predominantly by the energy loss from the lowest modes (dipolar modes), $N = 3$ (for $n_x = n_y = n_z = 1$), and where higher modes (multipolar) are involved $N = 6$ ($n_x = n_y = 1$, $n_z = 2$) or higher apply. The constants a and b have been calculated as 39 and -8.0, respectively, based on $N = 3$ and from the experimental data of gold (Kim et al. 2011).

Interestingly, the second term appears to be a quantum effect term by the presence of (h/mc), mainly found in the Compton effect. This could be suggesting a new form of photon scattering which sets in when the particle size falls below certain values. In the Mie theory (Mie 1908), however, photon scattering is expected to vanish as the particle size reduces but Pinchuk et al. (2004) have assumed a new kind of scattering to account for the increasing $\Delta\lambda$. While the prediction of the proposed model also suggests new scattering effect, whether it should be the electrons or the photons being scattered would call for further consideration, for a conclusive assessment of the conflicting ideas. The term (h/m) can be expressed in terms of the electron velocity at the Fermi energy (v_{F},), according to Kittel (1986).

$$\frac{h}{m} = 2\pi v_F \left(\frac{1}{3\pi^2\rho}\right)^{1/3},$$

where ρ is the electron density.

When inserted into Eq. 20, we get the expression of Eq. 21.

$$\lambda_2 - \lambda_1 = \Delta\lambda = a\gamma \frac{\lambda_{\max}^2}{2\pi c} + b\frac{\lambda_{\max}^2 (2\pi^2)N}{4\pi R^2 (3\pi^2\rho)^{1/3}} \frac{v_F}{c}. \quad (21)$$

In this form, Eq. 21 is very similar to Eq. 2 and is considered a proof that the inverse effect of size, for which Pinchuk et al. (2004) invoked the electron-surface scattering (for sizes below ~20 nm), is obtainable without starting from any of the controversial phenomenological factors such as the surface scattering, new surface Eigenmodes or chemical effect. Because of the Compton effect-like term, it is possible that energy transfer to the electrons by the scattered photons may lead to unprecedented new Eigenmodes as predicted in Fig. 2iib. Thus, while a new form of scattering and new Eigenmodes are predicted to be part of small size effect the model does not find a reason why they should be the basis for the proof of the inverse seize effect. On scrutiny, the first and the second terms of Eq. 21 (due to γ and R, respectively) exhibit opposite effects on the absorption bandwidth ($\Delta\lambda$), which would lead to a minimum value for $\Delta\lambda$ in the anomalous region. As the NP size changes, one term reduces as the other increases, depending on the direction of change of the NP size. They express effects of different size regimes, about a minimum, which lead to size-dependent anomalous bandwidth behavior already observed in the experimental results for gold (Link and El-Sayed 1999a, b).

Test results

Absorption peak positions and modes

The graphs of Fig. 2i and ii, derived from Eq. 16, show good predictions of the expected absorption signatures and the regions of strong light absorption by Ag, Au, and Cu as well as the difference in their absorption features. For Ag, the strongest absorption peaks occur in the wavelength range of 398–472 nm, far from the interband transition peak which is the low absorption appearing at 355 nm. Like the model of Eq. 1, the NP size only influences the peak intensity while ω_p brings the peak shift. The peak strengths vary with the wavelength. For Au and Cu, the absorption locations also occur at the expected wavelengths of ~522 and 583 nm, respectively. Similarity is evident in the overlap of the IB and CB modes in Au and Cu NPs, unlike in Ag. There is strong overlap of the IB and CB absorption whose resolution and intensity also change with the refractive index of the medium, Fig. 2ib, ic and iib, iic. As the refractive index of the medium changes from 1.0 to 1.33, the resolution is enhanced by red shifting the CB mode, both in Au and Cu. However, while the intensity of the red shifted peaks increases for Au it is severely quenched in Cu. For Ag, only the absorption intensity increases. This points out the similarity and difference in the influence of their IB electrons. Because the optical spectroscopy combines the influence of valence and the CB electrons, the model provides opportunity to see where there is strong and weak influence of the overlap of the IB and the CB electrons.

The first sign of the anomalous or switching behavior in the absorption bandwidth of metal NPs is revealed in Fig. 2iib, iic. There are two well-resolved absorption bands of inverted frequency effects, with a sharp transition point. Thus, the model reveals a plasmon frequency (ω_p)-dependent property inversion, where the strongest mode in one absorption band becomes the weakest in the other band. For Au, the transition point appears around 583 nm in the medium of refractive indices of 1.0 and 1.33 nm but shifts to 549 nm when the index is 1.5. In copper, it occurs around 618 nm for the indices of 1.0 and 1.33 nm. Also, the number of strong modes is higher in one band (higher energy side) than the other. In the shorter wavelength regime, increase in ω_p (corresponding to reducing particle size in the quantum context) leads to an increase in the number of observable modes and broadening. This, in one way, confirms the emergence of new surface modes, as expressed by Kawabata and Kubo (1966) who have attributed the cause of spectral broadening to new additional modes. The occurrence of multipolar modes (split in the absorption peaks) is also seen to be predicted in Au and Cu, at low ω_p, but not in Ag, Figs. 2 and 3. From Fig. 3, the anomalous bandwidth behavior in gold is evident and well expressed. It shows the dependence of bandwidth on the plasmon

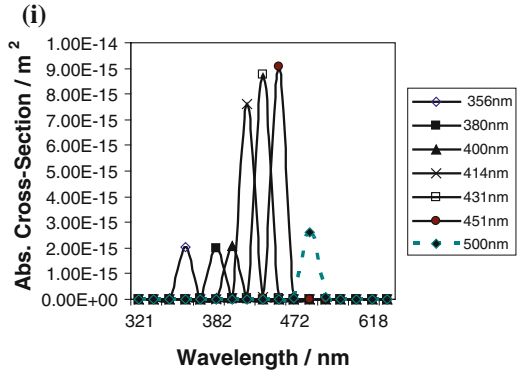

(a) Ag, plasmon resonance frequency range corresponding to λp (356 – 500nm)

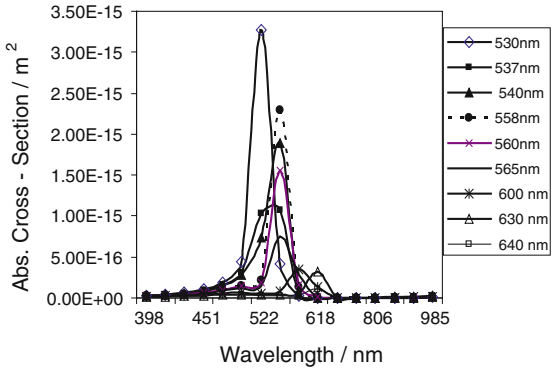

(b) Au, plasmon resonance frequency range corresponding to λp (530 – 640nm)

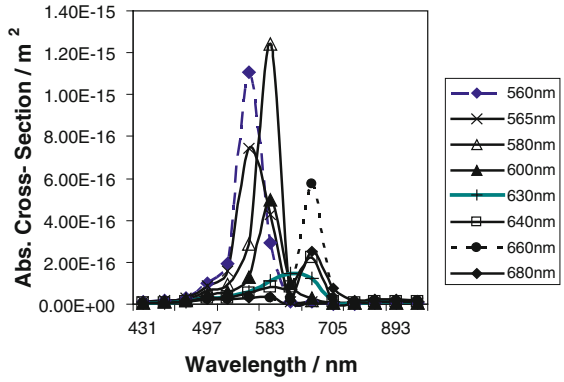

(c) Cu, plasmon resonance frequency range corresponding to λp (560 – 680nm)

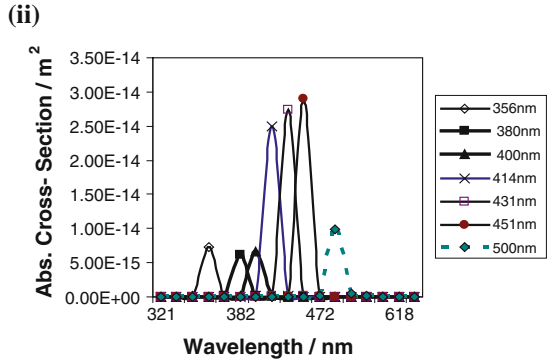

(a) Ag, plasmon resonance frequency range corresponding to λp (356 – 500nm)

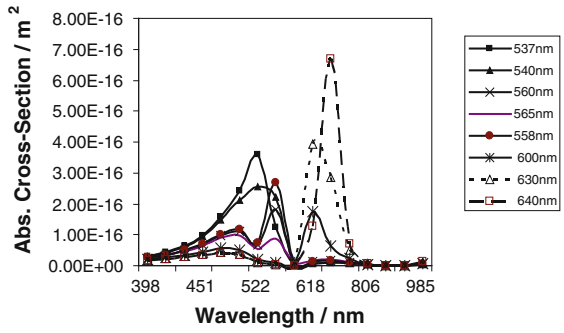

(b) Au, plasmon resonance frequency range corresponding to λp (537 – 640nm)

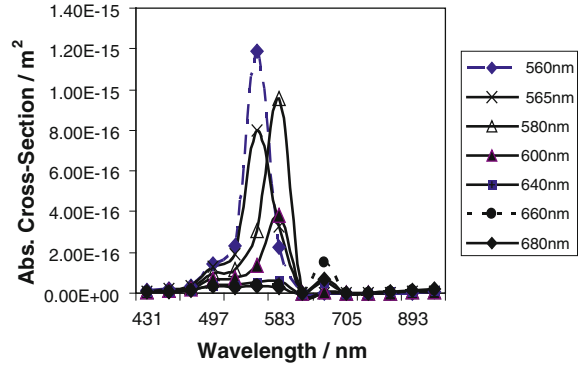

(c) Cu, plasmon resonance frequency range corresponding to λp (560 – 680nm)

Fig. 2 Absorption modes in a medium of refractive index **i** n = 1.0 and **ii** n = 1.33: **a** silver, **b** gold, and **c** copper

resonance frequency where a decrease is seen in the bandwidth at first, as the frequency increases, before it starts increasing again. This suggests a turning point value for the plasmon resonance frequency, which should correspond to some NP size. While this occurrence is predicted from the absorption cross section Eq. 16, it has been confirmed in the experimental bandwidth results for gold by Link and

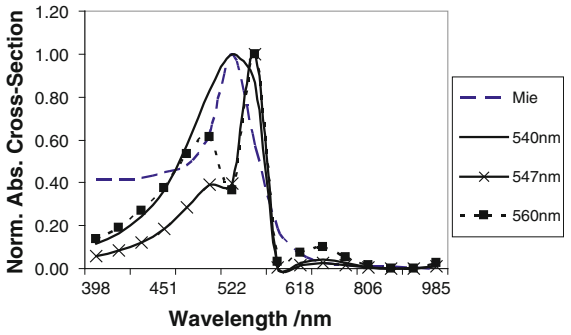

Fig. 3 Eigenmodes in gold for plasmon frequencies corresponding to the range (λ_p = 540–560 nm) against the Mie model

El-Sayed (1999a, b) and can be analyzed further through the derived bandwidth Eq. 20. While the same is predicted for copper, the model's absorption cross section Eq. 16 fails to detect this bandwidth behavior in Ag, Fig. 2i, ii.

The predictions, in essence, suggest that the peak shifts, bandwidth broadening, the emergence of new modes and the occurrence of multipolar modes are brought majorly by the internal mechanisms which depend on how strong the interaction between the IB and the CB electrons is. The absence of such features in Ag, based on the used data, may be suggesting low IB effect in Ag and, therefore, any observation of such features from experiment may be attributed to external damping factors, such as the adsorption of molecules on the silver NPs as observed in a report by Link and El-Sayed (1999a, b) as well as by Persson (1993). On its part, the Mie's dipole approximation model of Eq. 1 (Mie 1908) does not predict the occurrence of multipolar modes, which it considers a large-NP size effect whose predictive parameters are only found in the full Mie theory. There is no contradiction with our model on this, as even in the proposed model of this article the multipolar modes occur only from certain frequencies, basically low ω_p, which correspond to increased NP sizes in the quantum context. Peak shifts are also predicted with the changing frequency (ω_p), with every peak position obtainable over a range of plasmon frequencies $\Delta\omega_p$, which results into a range of excitable Eigenmodes, Fig. 4a, b, c. This depends on the kind of damping in the metal NP, as resonance peak height depends on whether the damping is light or heavy in a system. For Eq. 1, there is no parameter for the shifting of a peak, except when the refractive index of the medium is changed. In general, low

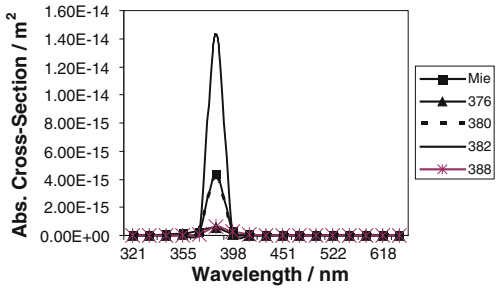

(a) Silver in ref. index 1.0 Plasmon resonance frequency range corresponding to λp = 376-388nm

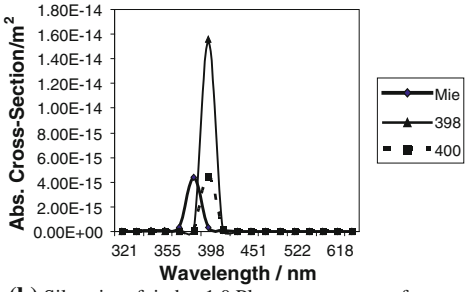

(b) Silver in ref. index 1.0 Plasmon resonance frequency range corresponding to λp (398-400nm)

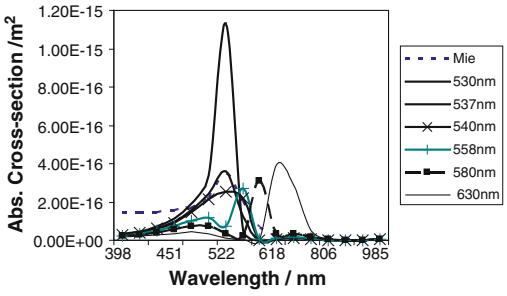

(c) Gold in ref. index 1.33 Plasmon resonance frequency range corresponding to λp = 530-580nm

Fig. 4 Eigenmodes at every peak position

damping resonances are difficult to tune in resonating systems, therefore, the peak intensities expected experimentally would be the medium size dumping peaks and they are expected to be influenced by the methods of synthesis of the metal NPs.

From Fig. 4a, b and c, the mathematically predicted Eigenmode peaks for Ag occur at 382 and 398 nm in the plasmon frequency ranges corresponding to (λ_p = 376–388 nm) and (390–405 nm), respectively, in a medium of index 1.0. For Au, the absorption peaks occur at 522 nm for the plasmon range (520–540 nm), in a medium of index 1.33. There are modes which may not be experimentally observable because the model assumes a free electron model for the CB

electrons while in reality they are not practically free, especially when both the internal and the external damping are significant as in the case of gold and copper. For silver, while the intense modes seen in Fig. 4a, b are the ones in good agreement with the experimentally observed absorption of $\sim 1.6 \times 10^{-14}$ m^2 for the NPs of size ~ 10 nm (Jensen et al. 2000), the intensities in agreement with Eq. 1 are only realized when the plasmon frequencies, within the two ranges given earlier, correspond to λ_p at 380 and 400 nm, respectively. For gold, however, it is the mode at 537 nm which corresponds well both to the experimentally observed results and the model of Eq. 1. Based on this plasmon wavelength value for Au (537 nm), the model gives absorption cross section of 3.58×10^{-16} m^2 for the NPs of radius 10 nm, against 3.51×10^{-16} m^2 from Eq. 1. For the radius of 20 nm the model gives 2.88×10^{-15} m^2 against 2.81×10^{-15} m^2 from Eq. 1 and 2.93×10^{-15} m^2 from the Discrete Dipole Approximation by Jain et al. (2006).

Both blue and red shifts of the absorption peaks are also predicted for gold but this is found to be dependent on the frequency (ω_p). and the refractive index of the medium, This is confirmed by some of the experimentally obtained peak locations, such as the absorption of 13.5 nm size of Au whose peak location has been observed at 518 nm while size 6.4 nm has a red shift to 523 nm (Lee et al. 2004; Kim et al. 2011). Thus, the peak location alone can be elusive as an indicator of the NP sizes. For the absorption bandwidth, Fig. 5 shows the calculated variation of the absorption bandwidth with NP sizes of Ag, from Eq. 20. It shows the same trend observed in the experimental results for Au NPs (Link and El-Sayed 2000). While the experimental results show the turning point for Au NPs at size ~ 20 nm, the calculation approximates it at ~ 16.3 and ~ 9.87 nm for Ag.

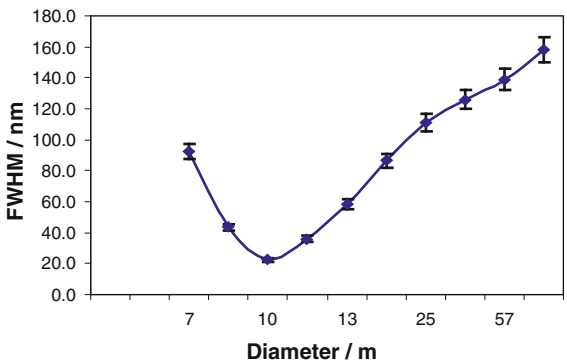

Fig. 5 Size dependence of the absorption bandwidth of silver NPs

Calculated NP sizes

From Eq. 20, the average NP sizes can be calculated from the experimental spectral parameters (λ_{max} and $\Delta\lambda$). However, given that the predicted spectral signatures for gold and copper show much overlap of the d-band and the CB absorption modes, as well as the increased broadening due to multipolar peaks (splitting of peaks at lower frequencies), compared to silver, the bandwidths of Au and Cu are, therefore, predominantly contributed to by the two effects. As a result, the effect of the first term (γ), is minimal and can be neglected for Au or Cu while setting $N = 6$ or 9, 12 or higher modes, especially at lower frequencies. On the other hand, because of the little effect of the d-band electrons in Ag and because of no internally triggered multipoles, both terms are considered equally significant to the bandwidth broadening and the dipole modes are assumed (thus, $N = 3$). With these assumptions, good agreement would be expected between the TEM measurements and the calculated values. On comparing our calculated average NP sizes of Ag with a range of sizes whose expected spectral features have been established by Solomon et al. (2007) good values have been realized. Where the absorption range of 395–405 nm, FWHM of 50–70 is reported to be expected for Ag NP sizes in the range 10–14 nm, our calculated average NP size (by Eq. 20) is 14.1 nm. Where the absorption occurs at 420 nm, FWHM 100–110 nm and the expected NP sizes given as 35–50 nm the calculated average size is 28.6 nm. For the absorption peak at 438 nm, FWHM of 140–150 nm whose expected NP size range is given as 60–80 nm the calculated value predicts 37.7 nm for $N = 3$ and 53.2 nm for $N = 6$. Such reported ranges are merely indicative of the probable sizes, however, most experimental results still show varied results which do not correlate well and this can be attributed to factors such as the kind of solvents used. For example, Ag whose TEM measurements and the absorption parameters have been reported by Shanmugam et al. (2006) as 6 nm with the absorption peak at $\lambda_{max} = 427$ nm and $\Delta\lambda = 112$ nm, the expected NP sizes, based on those spectral features should have

been in the range 35–50 nm and our model also predicts the size value of 31.7 nm.

For the gold sizes reported by Kim et al. (2011) as TEM size of 20.2 nm, spectral peak $\lambda_{max} = 525$ nm and $\Delta\lambda = 54.2$ nm the calculated size based on $N = 6$ is 23.4 nm. For TEM size of 21.0 nm, spectral peak $\lambda_{max} = 526$ nm and $\Delta\lambda = 58.8$ nm the calculated is 24.3 nm, these are very close values. However, for the NPs of TEM size reported as 24.4 nm, $\lambda_{max} = 530$ nm and $\Delta\lambda = 65.2$ nm the calculated value is 22.4 nm but for TEM size 29.4 nm, $\lambda_{max} = 532$ nm and $\Delta\lambda = 79.5$ nm the calculated value drops to 20.4 nm. As seen earlier, for gold there are frequencies where multipolar modes set in and they cause extra broadening whose bandwidth values would require correction or the use of $N = 6$ (or higher N modes for the multipolar modes). With $N = 6$, the calculated NP sizes for the last two cases of gold NPs above improve to 25.1 and 22.6 nm, respectively. Even as the model presents a good case of how the spectrometric results can be used to measure NP sizes, a few challenges of the influence of different experimental procedures and results are evident, especially where both the red and blue shifts occur as the NP size reduces. This is well expressed in the case of Au where the spectral features reported by Lee et al. (2004) for a TEM NP size of 6.4 nm, spectral peak λ_{max} (red shifted) of 523 nm, $\Delta\lambda = 89$ nm our calculated size is 14.7 nm and where TEM NP size is 13.5 nm, with λ_{max} (blue shift) = 518 nm and $\Delta\lambda = 77$ nm, the calculated value is 15.8 nm.

Conclusion

Normally, the optical spectroscopy combines the effects of IB and the CB absorption, and does not provide direct information about the influence of the IB electrons of a metal. The proposed model provides insight into the significance of the influence of the IB electrons on the optical absorption modes of metal NPs and reveals the possible cause of the unresolved conflicts about the anomalous behavior of the NP sizes below 50 nm. Considering the approximations made in the cause of the derivation of the model, yet very good agreement is still realized between the TEM results and the calculated NPs sizes, the model is a good tool for establishing NP size from the correlation of the spectroscopic parameters, mainly the wavelength at maximum absorption and the bandwidth.

Acknowledgments We acknowledge and thank Physics department, office of the Dean (SPAS), Graduate School-Kenyatta University, for the support we received in the course of this study.

References

Etchegoin PG, Le Ru EC, Meyer MJ (2006) An analytic model for the optical properties of gold. J Chem Phys 125:164–170

Gharibshahi E, Saion E (2010) Quantum mechanical calculation of the optical absorption of silver and gold nanoparticles by density functional theory. Phys Int 1:157–164

Grant I, Phillips W (1975) Electromagnetism. Wiley, New York

Jain P, Lee K, El-Sayed I, El-Sayed M (2006) Calculated absorption and scattering properties of gold nanoparticles of different size, shape, and composition; application in biological imaging and biomedicine. J Phys Chem B 110:7238–7248

Jensen T, Malinsky M, Hayne C, Duyne R (2000) Nanosphere lithography: tunable localized surface plasmon resonance spectra of Ag NPs. J Phys Chem B 104:10549–10556

Johnson P, Christy R (1972) Optical constants of the noble metals. Phys Rev B 6:4370–4379

Kawabata A, Kubo RJ (1966) Electronic properties of fine metallic particles: plasma resonance absorption. Phys Soc Jpn 21:1765–1772

Kim J, Bac L, Kim J (2011) Size, optical and stability properties of gold nanoparticles synthesized by electrical explosion of wire in different aqueous media. Rev Adv Mat Sci 28:117–121

Kittel C (1986) Introduction to solid state physics. Wiley, New York

Kreibig U, Genzel L (1985) Optical absorption of small metallic particles. Surf Sci 156:678–700

Kreibig U, Vollmer M (1995) Optical properties of metal clusters. Springer, Berlin

Lee C, Kim S, Yoon C, Gong M, Choi B, Kim K, Joo S (2004) Size-independent adsorption of 1,4-phenylenediisocyanide onto gold Np surfaces. J Coll Interface Sci 271:41–46

Link S, El-Sayed M (1999a) Size and temperature dependence of the plasmon absorption of colloidal gold nanoparticle. J Phys Chem B 103:4212–4217

Link S, El-Sayed M (1999b) Spectral properties and relaxation dynamic of surface plasmon electronic oscillations in gold and silver nanorods. J Phys Chem B 103:8410–8426

Link S, El-Sayed M (2000) Shape and size dependence of radiative, non-radiative and photothermal properties of gold nanocrystals. Int Rev Phys Chem 19:409–453

Mie G (1908) Beitrage Zur optik truber medien. Ann Phys (Leipzig) 25:377

Nordlander P, Prodan E (2003) Electronic structure and optical properties of metallic nanoshells. Cond Matter 0301289, 256–261

Patil S (1984) Elements of modern physics. Tata Mcgraw-Hill, New Delhi

Persson NJ (1993) Polarizability of small spherical metal particles: influence of the matrix environment. Surf Sci 281:153–162

Pinchuk A, Plessen G, Kreibig U (2004) Influence of interband electronic transitions on the optical absorption in metallic nanoparticles. J Phys D 37:3133

Saleh B, Teich M (1991) Fundamentals of photonics. Wiley, New York

Shanmugam S, Viswanathan B, Varadarajan T (2006) A novel single step chemical route for noble metal nanoparticles embedded organic-inorganic composite films. Mater Chem Phys 95:51–55

Solomon S, Bahadory M, Jeyarajasinglam A, Rutkowsky S, Boritz C (2007) Synthesis and study of silver nanoparticles. J Chem Ed 84:322–325

Yeshchenko O, Dmitruk I, Dmytruk A, Alexeenko A (2007) Influence of annealing conditions on size and optical properties of copper nanoparticles embedded in silica matrix. Mater Sci Eng, B 137:247–254

Zharov V, Galitovsky V, Viegas M (2003) Photothermal detection of local thermal effects during selective nanophotothermolysis. Appl Phys Lett 83:4897–4899